Growth Mechanism and Surface Morphologies of $Sm_{1+x}Ba_{2-x}Cu_3O_{6+y}$ Thin Films

Yutaka Yoshida, Kimihiko Sudoh, Yusuke Ichino, Izumi Hirabayashi, and Yoshiaki Takai

***Abstract*—In order to obtain high quality multilayer $Sm_{1+x}Ba_{2-x}Cu_3O_{6+y}$ (SmBCO) coated conductors, it is indispensable to understand the surface growth mechanism of the SmBCO system. Using AFM, the step-and-terrace features due to 3D island growth are observed that are polygonal-like from the surface images. Steps and terrace width are approximately 1.2 nm in height and 30 nm in width, respectively. Spiral steps accompanied by screw dislocations were observed on the surface films of Ca doped SmBCO films. The spiral shapes of Ca doped SmBCO films are polygonal-like with width of $\sim$ 80 nm. Using Ca-doping, the surface morphology of the SmBCO films changes from 3D island growth mode to spiral growth, and contributes to the flat surface of the SmBCO-multilayers.**

***Index Terms*—Superconducting film, superconducting wires, surfaces, thin films.**

I. Introduction

THE application of high-temperature superconducting (HTS) materials in the field of electronic devices and coated conductors requires the manufacturing of the film with good superconducting and morphological properties. Recently, the rare earth-123 (RE-123) superconductors particularly $NdBa_2Cu_3O_{6+y}$ (NdBCO), which showed good Jc dependence on H and also high stability to atmospheric degradation, have emerged as an alternate for $YBa_2Cu_3O_{7-y}$ (YBCO) material in bulk form [1], [2]. Furthermore, with respect to YBCO, NdBCO thin films exhibit better crystallinity and surface morphology [3].

We have reported the superconducting properties of NdBCO films deposited by the metal organic chemical vapor deposition (MOCVD) method. Transmission electron microscopy (TEM) observation of the NdBCO films revealed that the phase separation caused by the Nd-Ba substitution, was the cause of the different behavior of their electrical and magnetic properties [4]. Therefore, we have studied the effect of this substitution on the properties of RE-123 thin films from the viewpoint of the difference in the ionic radius and the substitution value x in the $RE_{1+x}Ba_{2-x}Cu_3O_{6+y}$ system [5]. $Sm_{1+x}Ba_{2-x}Cu_3O_{6+y}$ (SmBCO) films were found to show a zero resistance temperature (T_c) of $\sim$ 91 K and critical current density (J_c) of $\sim$ 8 MA/cm^2 at 77 K [6]. The J_c of SmBCO films deposited using $x = 0$ and $x = 0.04$ decreased with increasing film thickness. However, the J_c of the films deposited using $x = 0.08$ was $\sim$ 3 MA/cm^2, and increased with the film thickness. This makes the $RE_{1+x}Ba_{2-x}Cu_3O_{6+y}$ system a very interesting material for the coated conductor, and it is important to get a clear understanding of the film growth and the surface growth mechanism.

There are many reports concerning the surface morphologies of HTS thin films. From the surface morphology of YBCO films fabricated by MOCVD, we found the existence of a quasi liquid layer on the growing surface above 750°C and proposed the possibility of the vapor-liquid-solid growth mode [7].

When YBCO films were prepared on cube textured Ag tape, numerous spiral steps accompanied by screw dislocations were observed, and many particles were observed on the terrace surface of the spiral steps. They gradually became smaller and concentrated at the step edge with increasing heat treatment temperature. From the results of atomic force microscopy (AFM) and scanning Auger microscopy (SAM), we found that Ag segregated to the surface of film and acted as a surfactant during the growth of YBCO film [8].

In this paper, we fabricated high critical current (I_c)-SmBCO films by the pulsed laser deposition (PLD) technique for coated conductors. In particular, we discuss the surface morphology of the films with Sm-Ba substitution quantities. Furthermore, the AFM images of Ca-doped SBCO films are discussed for the high I_c SBCO-multilayers.

II. Experimental

The SmBCO and Ca-doped SmBCO thin films were grown on MgO (100) substrates by the PLD technique using a 193 nm ArF excimer laser. The energy density of the laser beam was about 1 J/cm^2 at the surface on the target. The ArF laser was operated at a repetition rate of 10 Hz. The substrate was placed at 50 mm above the laser target and the oxygen partial pressure was fixed at 50 Pa. The substrate temperature was set at 800–880 °C. At the end of the deposition the vacuum chamber was filled with pure oxygen to 2.7×10^3 Pa and the heater was switched off. Before the measurements, the SmBCO films were annealed at 350 °C for 1 hour in the flowing oxygen.

The crystal structure of the deposited films was examined by θ–2θ X-ray diffraction (XRD) method. In particular, the in-plane orientation of the films was determined by X-ray pole-figure measurements using the Schulz reflection method. The T_c of the grown films was measured by four-probe

Manuscript received August 5, 2002. This work was supported in part by New Energy and Industrial Technology Development Organization (NEDO) as a part of its Research and Development of Fundamental Technologies for Superconductor Applications Project under the New Sunshine Program administrated by the Agency of Industrial Science and Technologies M.I.T.I of Japan.

Y. Yoshida, K. Sudoh, Y. Ichino, and Y. Takai are with the Nagoya University, Department of Energy Engineering and Science, Nagoya 464-8603, Japan. (e-mail: yoshida@nuee.nagoya-u.ac.jp; sudo@ees.nagoya-u.ac.jp; y-ichino@mbox.media.nagoya-u.ac.jp; takai@nuee.nagoya-u.ac.jp).

I. Hirabayashi is with the Superconducting Research Laboratory-International Superconductivity Technology Center, Nagoya 456-8587, Japan (e-mail: hiraizum@istec.or.jp).

Digital Object Identifier 10.1109/TASC.2003.812008

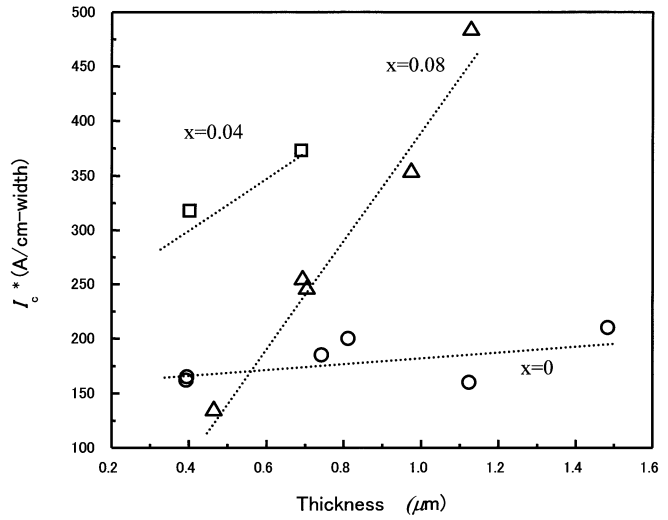

Fig. 1. Projected critical current (Ic^*) for 1 cm width as a function of SmBCOfilm thickness. The open circles, squares and triangles correspond to the data of $x = 0$, 0.04 and 0.08, respectively.

resistance measurement. The J_c was measured in the usual four-point probe configuration at 77 K and self field. Samples were patterned to form a microbridge 40–100 μm wide and 200 μm long using KrF excimer laser. The surface morphology of the films was investigated by AFM.

III. Results and Discussion

A. Superconducting Properties of SmBCO Films

We grew SmBCO thin films with c-axis orientation and cube on cube texture on MgO substrates, which have T_c higher than 91 K. For the SmBCO thin films fabricated at $x = 0.04$, the highest J_c (7.9 MA/cm^2) was obtained at the film thickness of 0.4 μm. The $x = 0$ and 0.04 films decreased as the film thickness is increased. Using the $x = 0.08$, we found that the J_c maintained the value over 2.9 MA/cm^2 for an increase of the film thickness. The maximum J_c of 4.3 MA/cm^2 was obtained at the film thickness of 1.1 μm at 77 K [6].

From the SmBCO film thickness dependence of the micro bridge J_c data, the I_c^* calculated for a hypothetical 1 cm wide tape is shown in Fig. 1. The I_c^* of SmBCO films using the $x = 0.04$ and 0.08 targets increased with the film thickness. The I_c^* of the $x = 0.08$ film with a thickness of 1.1 μm reaches a value of $\sim$ 480 A/cm-width.

B. Surface Morphology of SmBCO Films

It showed be possible to grow $\sim$ 300 nm SBCO thin films on the MgO with high J_c and I_c for the coated conductor. It is therefore important to get a clear understanding of the SmBCO film dependence on the Sm-Ba substitution quantities. Fig. 2 shows the AFM images of (a) SmBCO film deposited with $x = 0$, (b) SmBCO film deposited with $x = 0.08$ and (c) SmBCO film deposited with $x = 0.12$. The growth mode of the SmBCO films is different for different values of the substitution quantity, x; very smooth surfaces are obtained for Sm-rich SmBCO films,

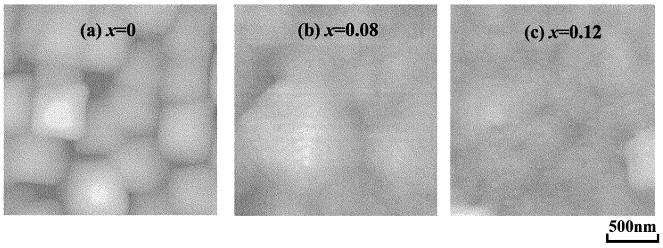

Fig. 2. AFM images of (a) SmBCO film deposited with $x = 0$, (b) SmBCO film deposited with $x = 0.08$ and (c) SmBCO film deposited with $x = 0.12$.

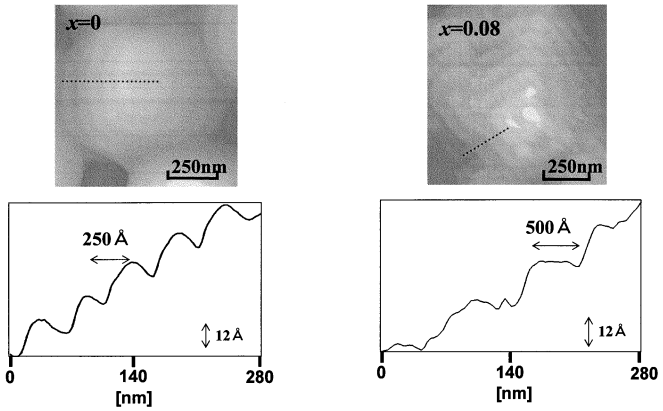

Fig. 3. AFM images and line scan profile of (a) a SmBCO film deposited with $x = 0$ and (b) a SmBCO film deposited with $x = 0.08$.

while the stoichiometric SmBCO films show 3D towers of unit cell height along the c-axis.

For the root mean-square (Rms) of surface roughness of the SmBCO films in the Fig. 2, the Rms value is $\sim$ 5 nm, $\sim$ 2 nm and $\sim$ 2 nm for the film deposited using the $x = 0$, 0.08 and 0.12, respectively. In fact, very smooth surfaces are obtained for Sm-rich SmBCO film.

We have used higher resolution AFM images to elucidate the origin of the change in surface morphology in the SmBCO films. Typical AFM images at higher magnification with their line scan profiles for SmBCO films deposited using $x = 0$ and $x = 0.08$ are shown in Fig. 3.Steps are approximately 1.2 nm in height, which agrees with the one unit cell height along the c-axis of the SmBCO. The shape of the growth steps for the stoichiometric films are rounded, as shown in Fig. 3(a), whereas the shape of those for the Sm-rich films are polygonal-like, as shown in Fig. 3(b).

Furthermore, in Fig. 3(a) the terrace widths of the each step are $\sim$ 25 nm, which is similar to the widths reported for YBCO films grown by PLD method [9]. The terrace widths of the Sm-rich SmBCO films are $\sim$ 50 nm, which is wider than that YBCO films. Fig. 4 shows the dependence of the terrace width on the x value in $Sm_{1+x}Ba_{2-x}Cu_3O_{6+y}$ films on MgO substrates from the AFM images. The terrace width increases as the Sm-Ba substitution quantities increase. It is concluded that the growth mode shifts from 3-dimentional island growth to atomically flat 2-dimentional layer-by-layer growth as the Sm-Ba substitution increased. We speculate that the surface growth mode change in the SmBCO lead to the high I_c SmBCO thick film.

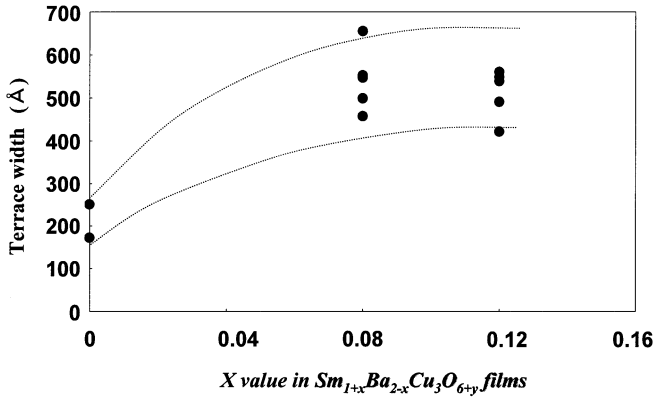

Fig. 4. Dependence of the terrace width on the x value in $Sm_{1+x}Ba_{2-x}Cu_3O_{6+y}$ films on the MgO substrates taken from the AFM images.

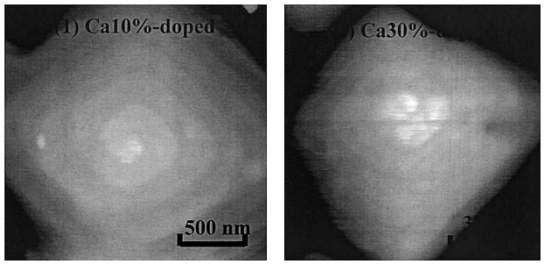

Fig. 5. AFM images of the $Sm_{0.9}Ca_{0.1}Ba_2Cu_3O_{6+y}$ films and the $Sm_{0.7}Ca_{0.3}Ba_2Cu_3O_{6+y}$ films showed in (1) and (2), respectively.

C. Surface Morphology of (SmCa)BCO Films

It is necessary to give insight into the mechanism controlling the grain boundary behavior for the higher I_c SmBCO thick films. The improvement of the grain boundary transport properties by doping, such as $YBa_2Cu_3O_{7-y}/(Y,Ca)Ba_2Cu_3O_{7-y}$ superlattices, is of great importance for application in coated conductors [10].

In this section, we discuss the growth of $(Sm,Ca)Ba_2Cu_3O_{6+y}$ ((SmCa)BCO) films for fabricating SmBCO/(SmCa)BCO multilayers. (SmCa)BCO films have the $T_{c,onset} \sim 80$ K and $T_{c,zero} \sim 40$ K. Fig. 5 shows the AFM images of a $Sm_{0.9}Ca_{0.1}Ba_2Cu_3O_{6+y}$ film and a $Sm_{0.7}Ca_{0.3}Ba_2Cu_3O_{6+y}$ film. Screw dislocations on the plate-like crystallites are observed in both the images. The spiral shapes of growth steps for the Ca- doped SmBCO films are polygonal-like.

Fig. 6 shows the terrace width versus for $(SmCa)Ba_2Cu_3O_{6+y}$ films on MgO substrates from the AFM images. The terrace width is ~ 90 nm, which is wider than that data of the SmBCO-PLD film. The terrace width increases with increasing Ca-dopant quantities.

The spiral morphology, whether it takes a circular or a polygonal form, is determined by the step energy. If we use the model of a Kossel crystal to calculate the thermodynamic properties of the crystal surface, Jackson' α-factor, which represents the lateral bonding energy between the growth units, determines the step roughness [11]. In previous work,

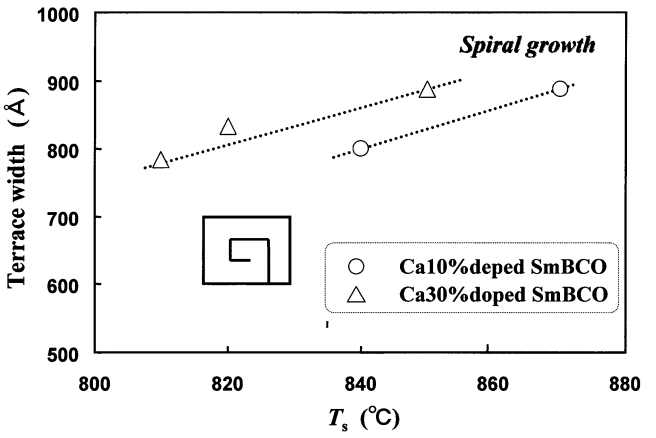

Fig. 6. Dependence of the terrace width on the substrate temperature for $(SmCa)Ba_2Cu_3O_{6+y}$ films on the MgO substrates from the AFM images. The open circles and triangles correspond to the data of the films fabricated using the $Sm_{0.9}Ca_{0.1}Ba_2Cu_3O_{6+y}$ target and the $Sm_{0.7}Ca_{0.3}Ba_2Cu_3O_{6+y}$ target, respectively.

we studied the growth mechanism of YBCO deposited by metalorganic (MO) chemical vapor deposition using the MO sources with and without fluorine [12]. As the results show, there is no difference in the terrace width dependence on the growth temperature between the two films using the different MO sources, while the different values of the α; value for the films were explained. In the case of the SmBCO film with Ca-doped quantities, the different behavior is not the α-factor but the terrace width. The spiral morphology is dominated not only by the value of α-factor and the terrace width but also by the kinetic effects which are represented by the magnitude of supersaturation, the driving force of the crystal growth. The effect of supersaturation, which is defined as the chemical potential ($\Delta\mu$) and the melting temperature (T_M) will be reported elsewhere.[13]

IV. Conclusion

High quality c-axis oriented SmBCO thin films were grown on MgO substrates by PLD. The superconducting properties of the films were $T_c \sim 91$ K and $J_c = 4.3$ MA/cm^2 (77 K, 0 T) with the thickness of 1.1 μm. The I_c^* of the $x = 0.08$ film with the thickness of 1.1 μm reached a maximum value of $\sim$ 480 A/cm-width.

From the AFM images of the SmBCO thin films, the terraces of the steps on the film surface were smooth, which is caused by growth mode shifts from 3-dimensional island growth to atomically flat 2-dimensional layer-by-layer growth as the Sm-Ba substitution is increased.

Furthermore, the surface growth of (SmCa)BCO thin films is discussed for fabricating a SmBCO/ (SmCa)BCO multilayer. The surface morphologies are drastically changed with Ca concentration in the (SmCa)BCO at the spiral step.

We presume that the surface growth mode change in the SmBCO lead to the high I_c SmBCO thick films, and the effect of the Ca-doped SmBCO layer between the SmBCO layers allow for deposition of thick films.

REFERENCES

[1] S. I. Yoo, M. Murakami, N. Sakai, T. Higuchi, and S. Tanaka, "Enhanced T_c and strong flux pinning in melt-processed $NdBa_2Cu_3O_y$ superconductors," *Jpn. J. Appl. Phys.*, vol. 65, pp. L1000–1003, July 1994.

[2] A. K. Dradhan, K. Kuroda, K. Nakao, and N. Kishizuka, "Magnetoresistence and magnetization studies of $Nd_{1+x}Ba_{2-x}Cu_3O_{7-y}$ single crystals," *Physica C*, vol. 272, pp. 161–168, Oct. 1996.

[3] M. Badye, F. Wang, Y. Kanke, K. Fukishima, and T. Morishita, "High-quality c-axis oriented superconducting $Nd_{1+x}Ba_{2-x}Cu_3O_{7-y}$ thin films deposited by the laser ablation method," *Appl. Phys.Lett.*, vol. 66, no. 16, pp. 2131–2133, Apr. 1995.

[4] Y. Kumagai, Y. Yoshida, M. Iwata, M. Hasegawa, Y. Sugawara, T. Hirayama, Y. Ikuhara, I. Hirabayashi, and Y. Takai, "Fabrication and characterization of $Nd_{1+x}Ba_{2-x}Cu_3O_7$ thin films deposited by metal-organic chemical vapor deposition using liquid state sources," *Physica C*, vol. 304, pp. 35–42, May 1998.

[5] K. Sudoh, Y. Yoshida, N. Matsunami, and Y. Takai, "Superconducting properties and surface morphology of $SmBa_2Cu_3O_{7-y}$ thin films," *Physica C*, vol. 357–360, pp. 1358–1360, Nov. 2001.

[6] K. Sudoh, Y. Ichino, M. Itoh, Y. Yoshida, Y. Takai, and I. Hirabayashi, "Correlation between film thickness and critical current density of $Sm_{1+x}Ba_{2-x}Cu_3O_{6+y}$ films deposited by pulsed laser deposition," Jpn. J. Appl. Phys., to be published.

[7] Y. Yoshida, Y. Ito, I. Hirabayashi, I. Hirabayashi, H. Nagai, and Y. Takai, "Surface morphology and growth mechanism of $YBa_2Cu_3O_{7-y}$ thin films by metalorganic chemical vapor deposition using liquid sources," *Appl. Phys. Lett.*, vol. 69, no. 6, pp. 845–847, Aug. 1996.

[8] M. Hasegawa, Y. Yoshida, M. Iwata, H. Akata, K. Higashiyama, Y. Takai, and I. Hirabayashi, "Evidence of mobile Ag and growth mechanism of $YBa_2Cu_3O_{7-y}$ films deposited on cube textured Ag tape by chemical vapor deposition," *Jpn. J. App. Phys.*, vol. 39, pp. 1719–1720, Apr. 2000.

[9] M. Hawley, I. D. Raistrick, J. G. Berry, and R. J. Houlton, "Growth mechanism of sputtered $YBa_2Cu_3O_{7-y}$ studied by scanning tunneling microscopy," *Science.*, vol. 251, pp. 1587–1589, Mar. 1991.

[10] G. Hammert, A. Schmehl, R. R. Schultz, B. Goetz, H. Bielefeldt, C. W. Schneider, H. Hilgenkamp, and J. Mannhart, "Enhanced supercurrent density in polycrystalline $YBa_2Cu_3O_{7-y}$ at 77 K from calcium doping of grain boundaries," *Nature*, vol. 407, pp. 162–164, Sep. 2000.

[11] K. A. Jackson, "Liquid metals and solidification," *Am. Soc. Metals.*, p. 174, 1958.

[12] Y. Yoshida, Y. Ito, Y. Yamada, H. Nagai, Y. Takai, and I. Hirabayashi I, "Surface morphology of $YBa_2Cu_3O_{7-y}$ films prepared by metalorganic chemical vapor deposition using liquid sources," *Jpn. J. App. Phys.*, vol. 36, pp. L1376–1379, Oct. 1997.

[13] K. Sudoh, Y. Ichino, Y. Yoshida, and Y. Takai, "Surface morphology of $(SmCa)Ba_2Cu_3O_{6+y}$ films deposited by pulsed laser deposition," *Physica C*, submitted for publication.